Dugaczyk, A., Law., A. W., & Dennison, O. E. (1982) *Proc. Natl. Acad. Sci. U.S.A. 79*, 71-75.
Gibbs, P. E. M., Ziclinski, R., Boyd, C., & Dugaiczyk, A. (1987) *Biochemistry 26*, 1332-1343.
Gibson, B. W., & Biemann, K. (1984) *Proc. Natl. Acad. Sci. U.S.A. 81*, 1956-1960.
Jagodzinski, L. L., Sargent, D. T., Yang, M., Glackin, C., & Bonner, J. (1981) *Proc. Natl. Acad. Sci. U.S.A. 78*, 3521-3525.
Law, W. S., & Dugaiczyk, A. (1981) *Nature 291*, 201-205.
Meloun, B., Moravek, L., & Kostka, V. (1975) *FEBS Lett. 58*, 134-137.
Morinaga, T., Sakai, M., Wegman, T. G., & Tamaoki, T. (1983) *Proc. Natl. Acad. Sci. U.S.A. 80*, 4604-4608.
Morris, H. R., & Greer, F. M. (1988) *Trends Biotechnol. 6*, 140-147.
Morris, H. R., Panico, M., & Taylor, G. W. (1983) *Biochem. Biophys. Res. Commun. 117*, 299-305.
Naylor, S., Fiendeis, A., Gibson, B. W., & Williams, D. H. (1986) *J. Am. Chem. Soc. 108*, 6357-6363.
Niall, H. D. (1973) *Methods Enzymol. 27*, 942-1010.
Pucci, P., & Sepe, C. (1988) *Biomed. Environ. Mass Spectrom. 17*, 287-291.
Pucci, P., Sannia, G., & Marino, G. (1983) *J. Chromatogr. 270*, 371-377.
Pucci, P., Carestia, C., Fioretti, G., Mastrobuoni, A. M., & Pagano L. (1985) *Biochem. Biophys. Res. Commun. 130*, 84-90.
Rhodes, C. J., Brennam, S. O., & Hutton, J. C. (1989) *J. Biol. Chem. 264*, 14240-14245.
Russel, J. H., & Geller, D. M. (1975) *J. Biol. Chem. 250*, 3409-3413.
Sargent, T. D., Yang, M., & Bonner, J. (1981) *Proc. Natl. Acad. Sci. U.S.A. 78*, 243-246.
Sell, S. (1982) in *Human Cancer Markers* (Sells, S., & Wahren, B., Eds.) pp 133-164, Humana Press, Clifton, NJ.
Takao, T., Hitouji, T., Shimonishi, Y., Tanabe, T., Inouye, S., & Inouye, M. (1984) *J. Biol. Chem. 259*, 6105-6109.
Tecce, M. F., & Terrana, B. (1988) *Anal. Biochem. 169*, 306-311.
Terrana, B., Tecce, M. F., Manetti, R., Ceccarini, C., Lamba, D., & Segre, A. L. (1990) *Clinical Chem. 36*, 879-882.
Turcotte, B., Wertin, M., Cheverette, M., & Belanger, L. (1985) *Nucleic Acids Res. 13*, 2387-2398.
Urano, Y., Sakai, M., Watanabe, K., & Tanaoki, T. (1984) *Gene 32*, 255-261.
Von Heijne, G. (1986) *Nucleic Acids Res. 14*, 4683-4690.
Watson, M. E. E. (1984) *Nucleic Acids Res. 12*, 5145-5164.
Yachnin, S., Hsu, R., Heinrikson, R. L., & Miller, J. B. (1977) *Biochim. Biophys. Acta 493*, 418-428.

Real-Time Analysis of the Assembly of Ligand, Receptor, and G Protein by Quantitative Fluorescence Flow Cytometry†

Shawn P. Fay, Richard G. Posner, William N. Swann, and Larry A. Sklar*

Cytometry, University of New Mexico, School of Medicine, Albuquerque, New Mexico 87131, and National Flow Cytometry Resource, M888 Los Alamos National Laboratory, Los Alamos, New Mexico 87545

Received August 31, 1990; Revised Manuscript Received February 8, 1991

ABSTRACT: We describe a general approach for the quantitative analysis of the interaction among fluorescent peptide ligands (L), receptors (R), and G proteins (G) using fluorescence flow cytometry. The scheme depends upon the use of commercially available fluorescent microbeads as standards to calibrate the concentration of fluorescent peptides in solution and the receptor number on cells in suspension. We have characterized a family of fluoresceinated formyl peptides and analyzed both steady-state and dynamic aspects of ligand formyl peptide–receptor interactions in digitonin-permeabilized human neutrophils. Detailed receptor-binding studies were performed with the pentapeptide *N*-formyl-Met-Leu-Phe-Phe-Lys-fluorescein. Equilibrium studies showed that GTP[S] caused a loss of binding affinity of approximately two orders of magnitude, from ~0.04 nM (LRG) to ~3 nM (LR), respectively. Kinetic studies revealed that this change in affinity was principally due to an increase in the dissociation rate constants from $\sim 1 \times 10^{-3}$ s^{-1} (LRG) to $\sim 1 \times 10^{-1}$ s^{-1} (LR). In contrast, the association rate constants in the presence and absence of guanine nucleotide ($\sim 3 \times 10^{7}$ s^{-1} M^{-1}) were statistically indistinguishable and close to the diffusion limit. In the presence of guanine nucleotide (LR), the kinetic data were adequately fit by a single-step reversible-binding model. In the absence of guanine nucleotides, not all receptors have rapid access to G to form the LRG ternary complex. Mathematically, those R that have rapid access to G are either precoupled to R or the association of G with R is fast compared to the association of L with R. The physiological consequences of coupling heterogeneity are discussed.

Cellular signal transduction proceeds through a sequence of events that is initiated via an extracellular ligand–receptor interaction. In neutrophils, activation involves the interaction of ligand–receptor (LR) complexes with guanine nucleotide binding proteins (G) (Okajima et al., 1985; Lad et al., 1985). Rapid interconversions among at least three distinct states of the receptor, which have been described as LR, LRG, and LRX (a desensitized form of the receptor), have been observed (Sklar et al., 1989). In the human neutrophil, the interactions of the formyl peptide receptor with its G proteins are reversible (Okajima et al., 1985; Sklar et al., 1987), but no systematic

†This work was supported by NIH Grants AII9032 and RR01315.
*To whom correspondence should be addressed.

0006-2960/91/0430-5066$02.50/0

measurements of the macromolecular assembly of the ternary LRG complex have been reported.

The interactions among ligands, receptors, and G proteins have been previously studied by radioligand techniques (Neubig et al., 1985; Kim & Neubig, 1985) and analyzed by a ternary complex formalism (De Lean et al., 1980; Lee et al., 1986) represented as a cycle of stepwise interactions among L, R, and G. Radioligand analysis has permitted direct observation of a few of the eight rate constants in the model (Contreras et al., 1986), and estimates of some of the others have been formulated in several systems, notably the α-(Neubig et al., 1988) and β-adrenergic receptor systems (De Lean et al., 1980). A technical limitation of radioligand technology is the separation step that is used to resolve the free radioligand from the receptor-bound radioligand. Because the affinity of the ternary complex is typically two orders of magnitude greater than the binary complex LR and because the dissociation rates of LR can be $\sim 1\ s^{-1}$ or greater, the detection of LR in radioligand assays has varied from system to system. In some cases, it has only been possible to study LR in competitive assays where the radioligand is a high-affinity receptor antagonist (Neubig et al., 1985).

We have previously described fluorometric methods used to study the binding of fluorescent peptides to cell-surface receptors at natural abundance (Sklar et al., 1984, 1987, 1989a). Several of these methods have the capacity to examine binding interactions continuously in homogeneous assays that require no separation step. Initially, these techniques were applied to whole cells (Sklar et al., 1984) and more recently to membranes and permeabilized cells (Sklar et al., 1987, 1989a) in which receptor–G protein interactions could be detected. The first report in permeabilized cells described the use of antibodies to fluorescein to discriminate the free and receptor-bound ligand (Sklar et al., 1987). However, this technique was not effective in examining association interactions directly and was more appropriate for dissociation. Preliminary analysis using fluorescence polarization detection did not provide an adequate signal-to-noise ratio to examine assembly as a function of ligand concentration (Sklar, 1987). This study was therefore undertaken to examine the dynamics of ligand, receptor, and G protein interactions in a quantitative manner. Permeabilizd neutrophils were used to study these interactions since this system allows resolution of the LRG and LR receptor states (Sklar et al., 1987).

Flow cytometry was chosen for these studies because its intrinsic ability to resolve free from bound ligand (Sklar et al., 1984, 1986; Sklar, 1987) makes it possible to examine ligand–receptor interactions over a wide range of ligand concentrations. In addition, a new effort at calibration of fluorescent reagents for flow cytometry was undertaken because the commercial standard previously available was not stable and is no longer being produced. Continuing experience with fluorescent peptides has made clear the need to insure quantitative transfer, detection, and recovery of the reagents. Finally, the development of a family of peptides for the formyl peptide receptor has revealed unique fluorescence properties for several members of the family that depend upon their length and the position of the chromophore (Sklar et al., 1990).

In the development of a calibration scheme, a fluorescein solution was used as a primary standard to confirm the number of fluorescein equivalents on commerical fluorescent microspheres and to determine the quantum yield of fluoresceinated formyl peptide ligands. The beads were used as a convenient daily standard for the fluorometric determination of fluorescent peptide concentration and the cytometric quantitation of the amount of bound receptor on cells. These calibration techniques provided a basis for studying the binding of ligand to receptor both at equilibrium and, kinetically, for LRG and LR receptor states. The results of these experiments provide insight into the regulation of ternary complex assembly and disassembly by a guanine nucleotide. In addition, these methods should find utility in the analysis of ligand binding and macromolecular assembly on cell surfaces.

Experimental Procedures

Materials

Neutrophils and Permeabilized Neutrophils. Human neutrophils were prepared by the elutriation method of Tolley et al. (1987) and permeabilized as described by Smolen et al. (1987) and modified for elutriated cells (Sklar et al., 1987). Briefly, stock solutions of digitonin (1 mg/mL in the intracellular buffer described below) were prepared daily. Neutrophils were suspended at 25×10^6 per mL in the same buffer and incubated for 25 min at 37 °C with 15 μg/mL digitonin.

Fluorescent Formyl Peptides. The hexapeptide CHO-Nle-Leu-Phe-Nle-Tyr-Lys-fluorescein[1] (FITC isomer I) was prepared as previously described (Sklar et al., 1984) or obtained from Molecular Probes (Eugene, OR). The tetrapeptide CHO-Met-Leu-Phe-Lys-fluorescein was obtained from Peninsula Laboratories (Burlingame, CA). The pentapeptide CHO-Met-Leu-Phe-Phe-Lys-fluorescein was prepared by the rapid mixed anhydride procedure (Muthukumaraswamy & Freer, 1987). Deprotection was accomplished with anhydrous HF containing anisole and dimethyl sulfide. Fluorescein was introduced by the reaction of the formylated peptide (0.1 mmol) with 1 equivalent of fluorescein isothicyanate (FITC isomer I) in 2 mL of saturated sodium bicarbonate and 0.5 mL of acetonitrile. Reaction was for 2 h at room temperature, and the reaction was stopped by the addition of 0.1 mmol of ethanolamine. Purification was by HPLC on a Whatman ODS-3 column with gradients of 0.1% trifluoroacetic acid/acetonitrile from 0 to 30%. Aliquots of these peptides were stored either in DMSO at concentrations ranging from 100 μM to 1 mM or as dry powders.

Buffers. The intracellular buffer described by Smolen et al. (1987) (100 mM KCl, 20 mM NaCl, 1 mM EGTA, 30 mM Hepes, pH 7.3) was supplemented with 0.1% BSA and 5 mM $MgCl_2$ and 1 mM PMSF to stabilize the peptide fluorescence. The concentration of Mg permits uncoupling of receptors and G proteins in the presence of a guanine nucleotide. We refer to this buffer as intracellular binding buffer (IBB). In earlier studies we used an extracellular buffer containing 30 mM Hepes, pH 7.0, 110 mM NaCl, 10 mM KCl, 1 mM $MgCl_2$, 10 mM glucose, and 0.1% BSA to stabilize the peptide against hydrophobic interactions with the cuvettes and transfer pipettes. We use this extracellular medium as a dilution buffer (DB) when transferring reagents.

Miscellaneous Reagents. The polyclonal antibody to fluorescein was prepared (Sklar, 1987) and its high-affinity binding quantitated as previously described (Levison et al., 1975). The formyl peptide antagonist tBoc-Phe-Leu-Phe-Leu-Phe was obtained from Vega Biochemicals (Tucson, AZ). GTP[S] was obtained from Sigma (St. Louis, MO). Fluorescent standard beads were obtained from Flow Cytometry

[1] Abbreviations: CHO, *N*-formyl group of formylated peptides; DB, dilution buffer; FITC, fluorescein 5′-isothiocyanate (isomer I); GTP[S], guanosine 5′-*O*-(3-thiotriphosphate); IBB, intracellular binding buffer; I_b/I_f, the ratio of the intensities of receptor bound and free peptide; Q_r, the ratio of the quantum yields of fluoresceinated peptide relative to free fluorescein; tBoc, *tert*-butyloxycarbonyl.

Standards Corp. (Research Triangle Park, NC).

Methods

Quantitation Strategy. Fluorescein is used as the primary standard to verify the calibration of fluorescent microbeads. The microbeads are used as daily standards to calibrate receptor numbers in flow cytometry and to standardize solutions of fluorescent peptides that are made fresh for each series of measurements.

Fluorescein Solutions. Fluorescein (sodium salt, Sigma F-6377 lot 107F-3469) was diluted in nanopure water to a theoretical stock concentration of 1 mM as determined by mass and diluted into IBB, pH 7.3. The absorbance was determined over a wavelength range of 600–400 nm with a Perkin-Elmer Lambda 4C spectrophotometer (Norwalk, CT). This procedure was then repeated with IBB, pH 9.0. The experimental extinction coefficient of 7.28×10^4 obtained in IBB at pH 7.3 was in good agreement with the published extinction coefficient of fluorescein of 7.25×10^4 in water at pH 8.0 (Nash, 1958) and within 10% of the values reported for FITC under analogous conditions (Haugland, 1989).

For fluorescence studies, the fluorescein solutions were diluted 1 to 100 in DB. Fluorescence was examined in the photon-counting mode in an SLM-Aminco 8000 or 8000C spectrofluorometer (Urbana, IL) outfitted with a cylindrical cuvette adapter (Sklar et al., 1990), cylindrical glass cuvette (Sienco, Morrison, CO), and a 2×5 mm stir bar (Bel-Art, Pequannock, NJ). The excitation was at 490 nm, and stray light was reduced with a 490-nm, 10-nm bandpass interference filter (Corion, Holliston, MA). The emission signal was monitored through a 520-nm, 10-nm band-pass interference filter (Corion) and a 3-70 OG Corning glass filter (Kopp, San Francisco, CA). To avoid phototube saturation and confirm linearity, samples were observed at several light levels.

Verification of Fluorescent Bead Calibration. Calibrated fluorescent bead standards, homogeneous in size and fluorescence, were obtained from Flow Cytometry Standards Corp. (Research Triangle Park, NC). The beads are solid with the nominal calibration reported as fluorescein equivalents per particle and suspended at nominal densities of 2×10^6/mL. As a standard, we used the largest and most highly fluorescent #1 beads (9.0-μm diameter, control no. 100188). Calibration involved counting the beads and then comparing their fluorescence to a known concentration of fluorescein. To count the beads, the stock solution was shaken vigorously, and 50 μL was transferred to a clear 1.5-mL Eppendorf tube in which the homogeneity of the solution was inspected. A total of 40 μL of these beads was transferred with a 100-μL Hamilton syringe into 20 mL of isotonic buffered saline and then immediately counted in a Coulter counter (Hialeah, FL) with the amplification and aperture current being set at 1 and 0.5, respectively. The concentration of the stock solution was determined to be 2.3×10^6 beads/mL.

To determine the specific fluorescence of the bead solution, 10 μL of bead solution was transferred via a 10-μL Hamilton syringe to a cuvette containing 200 μL of IBB. The specific fluorescein fluorescence was evaluated by reducing the pH below 5.5, where fluorescein is nonfluorescent, and was confirmed by determining the fluorescence of unlabeled beads. The residual signal (less than 10% of the signal), which represents stray light and background fluorescence of the latex particles and IBB, was substracted. A value of 2.3×10^6 fluorescein equivalents per bead was obtained.

Linearity of Bead Fluorescence. Flow Cytometry standard beads #2, #3, and #4 were calibrated relative to #1 beads by cytometric comparison on a Becton Dickinson Facscan flow cytometer (Mountain View, CA). A total of 50 μL of the bead suspension was diluted in 500 μL of IBB, pH 7.3. Forward-scatter and side-scatter parameters were adjusted to resolve the singlet bead population, and the mean channel of each bead species was quantified with the fluorescein (FL1) detector set at either 600, 730, or 800 V. The FL1 amplifier was set at 1.00 in all cases. Determination of the fluorescence of each bead at more than one detector setting allowed for the positioning of more than one bead fluorescence level on the same scale, as well as allowing for the normalization of fluorescence values obtained at different detector settings. Background fluorescence was determined at each detector setting with Flow Cytometry Standard Corp. #5 (blank) beads. On the basis of the fluorescence of #1 beads, the #2, #3, and #4 beads yielded values of 5.0×10^5, 2.3×10^5, and 5.3×10^4 fluorescein equivalents per bead, respectively, which were in reasonable agreement to the nominal values of 4.3×10^5, 1.8×10^5, and 6.4×10^4 fluorescein equivalents for #2, #3, #4 beads, respectively. The relative values were independent of instrument setting, validating the linearity of instrument response. Lot no. 110989 of #1 beads was found to agree within 3% of the original lot.

Calibration of Fluorescent Peptides. The formyl peptides are hydrophobic and relatively insoluble in aqueous media. Both absorbance and fluorescence measurements were determined on the same sample in the same polystyrene cuvette (Evergreen, Torrance, CA) to prevent peptide losses in the dilution or transfer steps. Peptides were diluted in IBB, pH 7.3, to a final concentration that was verified spectrophotometrically, on the basis an extinction coefficient of 8.1×10^4 for conjugated FITC at pH 7.3 (Mercola et al., 1972). The background fluorescence was determined with an identical polystyrene cuvette containing IBB. Peptide solutions of ~100 nM as verified by absorbance were prepared and compared directly to undiluted #1 beads, for which the fluorescein equivalent concentration was calculated to be 8.78 nM. In this manner, any difference in the quantum yield of the conjugated fluorophore as compared to the free fluorophore could be quantitated. Routine calibration of peptide solutions vs beads alleviated the need for the otherwise cumbersome daily standardization against fluorescein.

Spectrofluorometric Assays of Ligand Binding to Cell-Surface Receptors

Antibody Method. This assay has been described elsewhere (Sklar et al., 1989b). Permeabilized cells were suspended at 10^7/mL in IBB (pH 7.3), and 200-μL aliquots were placed in the stirred cylindrical cuvette of the SLM 8000 or 8000C under the same spectral conditions as described for fluorescein solutions. The fluorescence was monitored continuously following the addition of fluorescent peptide (Figure 1). Binding was allowed to proceed for the desired period of time, and antibody to fluorescein (2 μL, ~2500 nM) was added to the cuvette. Antibody binds and quenches the free fluorescent peptide within 1 s at a rate constant of $\sim 10^8$ M^{-1} s^{-1}. In contrast, antibody recognizes the receptor-bound hexapeptides with a half-time of ~300 s and with a rate constant of $\sim 10^5$ M^{-1} s^{-1}. Fluorescein on the shorter peptides is protected in the binding pocket of the cell-surface receptor and is entirely inaccessible to antibody to fluorescein (Sklar et al., 1990). For all the peptides, the addition of antibody spectroscopically discriminates the free and bound ligand. Because GTP[S] reduces the ligand affinity, the bound peptide is released and quenched by the antibody when GTP[S] is added. The fluorescence in the cuvette then falls to background (nonbound) levels upon the addition of GTP[S], confirming the

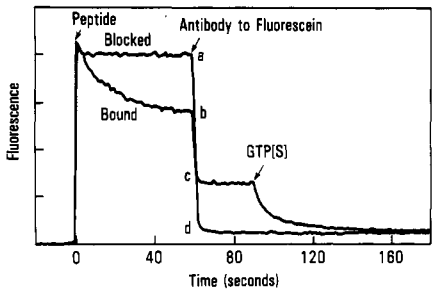

FIGURE 1: Spectrofluorometric detection of ligand binding and quenching. Permeabilized neutrophils were monitored spectrofluorometrically in a stirred cuvette with or without the blocking peptide. At time 0, the fluorescent pentapeptide was added. The antibody to fluorescein was then added after 60 s of incubation to quench the free ligand. The blocked sample traces the curve connected by *a* and *d*; the bound sample traces the curve connected by *b* and *c*. The fluorescence values *a*, *b*, *c*, and *d* can be related to the intensities and mole fractions of the fluorescent ligand according the following scheme. I_f is the intensity of free peptide; I_b is the intensity of cell-bound peptide; I_a is the intensity of antibody-bound peptide; and X_b is the mole fraction of cell-bound peptide. Then *a* represents free ligand with intensity I_a; *b* represents a combination of free ligand and quenched bound ligand where the intensity is given by $I_f(1 - X_b) + I_bX_b$; *c* represents a combination of receptor-bound ligand and antibody-bound ligand, the intensity being given by $I_bX_b + I_a(1 - X_b)$; and *d* represents the ligand bound to antibody where the intensity is I_a. By rearrangement and substitution, the residual fluorescence of the bound ligand I_b/I_f is given by $I_b/I_f = [(b - a)(a - d)/a(a - b + c - d)] + 1$ (eq 2). The GTP[S]-dependent decrease in fluorescence confirms that the cells were permeabilized.

extent of permeabilization of the cells.

Quenching within the Receptor Binding Pocket. As reported earlier (Sklar et al., 1990), the shorter peptides are quenched by their interaction with the binding pocket of the formyl peptide receptor, while the fluorescein on the hexapeptides is outside of the binding pocket. Because of the quenching, the change in quantum yield must be taken into account in the cytometric quantitation. As described in the legend to Figure 1, the antibody to fluorescein is used in the evaluation of the relative quantum yields of the free and bound ligand.

Cytometric Binding Assays

Equilibrium Binding Assays. The cytometric binding assays and their analysis follow the principles described for intact cells with the use of a Facscan flow cytometer (Sklar et al., 1984). A suspension of permeabilized neutrophils (10^6/mL) in freshly filtered IBB, pH 7.3, was equilibrated in the presence of calibrated solutions of the fluorescent peptide (nominal concentrations ranging from 0.01 to 30 nM) for at least 1 h at room temperature in the presence or absence of GTP[S] ("bound" samples). Control ("blocked") samples were made by suspending cells in IBB to which had been added excess nonfluorescent blocking peptide. As blocking peptides, we have used the agonists CHO-Met-Leu-Phe-Phe and CHO-Nle-Leu-Phe-Nle-Tyr-Lys (10^{-6} M) as well as the antagonist tBoc-Phe-Leu-Phe-Leu-Phe (4×10^{-5} M) with comparable results. In all cases, the blocking solution is filtered prior to cell addition. It is our experience that the presence of an insoluble peptide particulate in the concentrated peptide suspensions distorts the cytometric analysis.

Histograms of the individual suspensions were acquired at room temperature in the cytometer, and data were expressed as the mean fluorescence channel of the cell suspension. Specific binding was calculated from mean fluorescence channel values of the bound sample minus the mean of the blocked samples.

Calibration of Ligand Bound per Cell. For each ligand concentration, the mean ligand binding per cell, *B*, in the cell suspension was measured with the following formalism. The mean fluorescence channel number of ligand binding to the cells, *M*, was first determined. In order to convert the mean fluorescence channel number to fluorescein equivalents per channel requires a comparison with microbeads (typically #4 beads, where the factor *F* represents fluorescein equivalents/channel of the bead standard). To convert from fluorescein equivalents per channel to fluorescent peptide equivalents per channel, two additional pieces of information are needed: the ratio of the quantum yields of the free fluorescent peptide as compared to the free fluorescein (Q_r = 0.82, as determined from absorbance and fluorescence measurements described above) and I_b/I_f, the relative intensity of the receptor bound as compared to the free ligand in solution (Figure 1). The calculation of the average quantity of peptide bound to receptor per cell is given by

$$B \text{ (in ligand bound per cell)} = M \text{ (in mean channels/cell)} \times F \text{ (in fluorescein equivalents/channel)} \times 1/Q_r \times I_b/I_f \quad (1)$$

Free Ligand in Equilibrium Binding Experiments. Direct measurement of the concentration of free peptide in binding experiments was made to verify the amount of residual ligand after binding. Aliquots (200 μL) of equilibrated samples were removed prior to cytometric analysis and transferred to cylindrical cuvettes. The microcuvettes were seated in 96-well ELISA plates (Nunc, Thousand Oaks, CA), placed on carriers, and centrifuged at approximately 150*g* for 10 min sediment cells in suspension. The fluorescence of these samples was examined directly and their concentration then determined by comparison to microbead standards in solution.

Kinetic Cytometric Analysis. Kinetic measurements of ligand binding to the neutrophil formyl peptide receptor by flow cytometry were performed with the same principles of sample preparation and data analysis as in the equilibrium measurements. Cell suspensions, equilibrated at 37 °C for 10 min, were exposed to a calibrated solution of peptide (10 μL of peptide to 1 mL of 10^6 cells/mL), quickly vortexed, and then immediately placed on the cytometer, the sample temperature being regulated with a water jacket to 37 °C. In order to acquire binding data kinetically, repetitive histograms were acquired sequentially at intervals of 15–60 s, which was varied according to the steepness of the binding curve. Individual concentrations were repeated in duplicate in the presence and absence of guanine nucleotides for both "bound" and "blocked" cells. Typically, three or four concentrations of ligand ranging between 0.5 and 5 nM were tested in a single experiment. Histograms of 2000 cells were acquired in 3 s, the middle of the interval being picked as the time of acquisition. Because there is variability from sample to sample in the midpoint of data acquisition, specific binding was calculated by fitting the "blocked" sample data with a double-exponential curve and subtracting the calculated mean channels point by point from the "bound" samples (see Figure 5). Kinetic measurements of the dissociation of the bound ligand from its receptor were performed by diluting 100-μL aliquots of cells bound to equilibrium with 0.5 nM peptide into 900 μL of IBB containing blocking peptide or IBB containing blocking peptide and GTP[S], quickly vortexing, and then immediately placing the sample on the cytometer. Kinetic data were acquired as explained above.

Analysis of Binding Data. Equilibrium binding data were analyzed by nonlinear regression of bound peptide as a function of free peptide by the Graph Pad computer program (Motulsky, 1987). In the presence of saturating concentrations

Scheme I

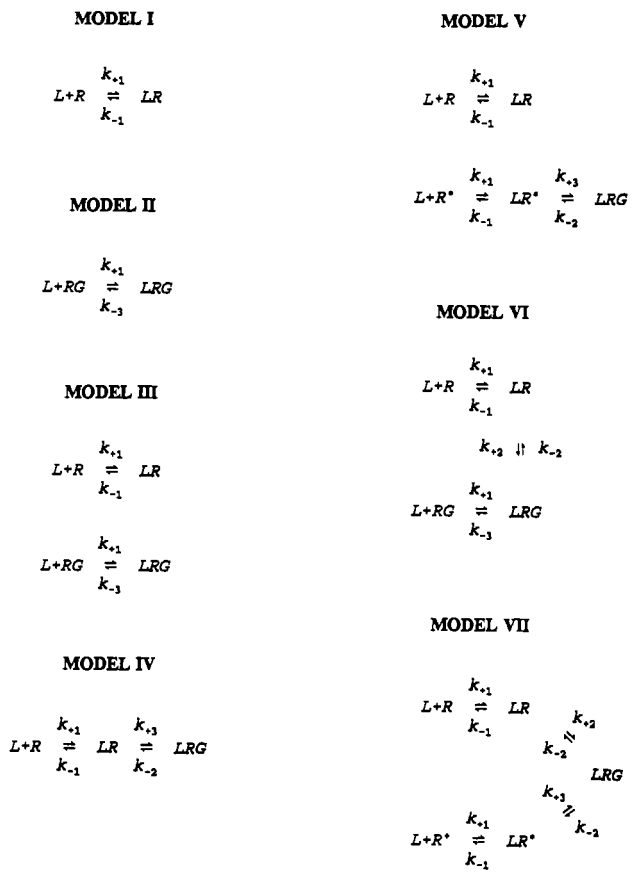

of guanine nucleotides (100 μM GTP[S]), data were fit to a single site (single rectangular hyperbola); in the absence of guanine nucleotides, data were fit to two independent sites (double rectangular hyperbola).

Binding models relevant to the ternary complex analysis were evaluated for kinetic experiments performed in the presence or absence of guanine nucleotides. These models are shown in Scheme I. The coupled differential equations that describe ligand binding for each of the models were solved numerically by the Gears method by using the Los Alamos National Mathematics Library routine SDRVB. Parameter estimates were obtained by using the International Mathematics and Statistics Library routine ZXSSQ based on the finite difference Levenberg–Marquardt algorithm for solving nonlinear least-squares problems. The analysis was performed on a Cray YMP supercomputer at Los Alamos National Laboratory.

In the presence of guanine nucleotides, kinetic and equilibrium data were fit to the single-step reversible-binding model (Model I). Data obtained in the absence of nucleotides were fit to one of the six models described below and optimized simultaneously with the single-step model for data in the presence of nucleotides. Model II is single-step reversible binding in which G is physically coupled to R. Model III involves two simultaneous single-step reversible interactions in which R is partitioned between precoupled and uncoupled forms. Model IV consists of a sequential two-step reversible binding in which L first binds to R and then LRG is formed in a second step. Model V is a combination of Models III and IV in which R is partitioned among receptors that couple (R*) or do not couple to G. Model VI represents three of the four sides of the complete cyclic ternary complex model. Model VII is a variation of Model VI in which all R are initially uncoupled from G. Upon binding of L, some R can couple rapidly with G while others (R*) couple with G slowly. The adequacy of each model was judged on χ^2 values, systematic errors, the agreement of both equilibrium and dissociation behavior with direct measurement, and the consistency of receptor sites predicted in the presence and absence of guanine nucleotides. In each model, the association rate constants of L with R or RG are assumed to be the same. Allowing for two independent rate constants for association did not result in a significant improvement in the fits (not shown). In judging the χ^2 criteria, it is worth noting that the nucleotide data sets are fit to the same single-step mechanism for each model and that the contribution of the nucleotide data set to χ^2 is relatively model insensitive.

Results

Calibration

Fluorescein. In order to achieve consistency in fluorescence measurements, calibration was made in terms of free fluorescein equivalents. The difficulties with this approach are the environmentally sensitive absorbance and fluorescence properties of fluorescein (Nash, 1958). Since the extinction coefficient of fluorescein is known to within ~10% as a function of pH in aqueous media, the calibration is accurate in this range. These issues are discussed in the description of the bead standards (Flow Cytometry Standards Corp., 1988).

Commercial Beads. We verified the behavior of the bead standards in terms of their absolute brightness compared to fluorescein and their relative brightness compared to one another. Uncertainties in these measurements are the extinction coefficient of fluorescein and the bead density. The pH behavior of the beads and the fluorescein standards are comparable. For semiquantitative purposes, the beads can be used as sold.

Fluoresceinated Peptides. Peptide solutions were examined by absorbance spectroscopy with an extinction coefficient of 8.1×10^4 at pH 7.3, a value typical of FITC and several model compounds (Mercola et al., 1972). The absorbance spectra of the peptides were all comparable. The fluorescence of the same peptide solutions in the same cuvettes was calibrated in free fluorescein equivalents vs beads in order to calculate the relative quantum yield of the fluorescent ligands as compared to free fluorescein. Q_r values of the tetra-, penta-, and hexapeptides were not statistically different from each other: 0.89 ± 0.05, n = 7; 0.72 ± 0.13, n = 3; and 0.79 ± 0.09; n = 4, respectively. The Q_r calculated from multiple determinations for all the peptides yielded a mean value of 0.82 relative to free fluorescein with a standard deviation of approximately 10%. The uncertainties arise from the relative difficulty in making absorbance measurements on solutions below 0.01 OD.

Q_r values were consistent with fluorescence lifetime measurements,[2] which showed that both modulation and phase measurements of fluorescence lifetimes of three of the fluorescent peptides were not statistically different. This might be expected, since in all cases these peptides were labeled with FITC isomer I, which was conjugated to each peptide through a carboxy-terminal lysine residue.

Fluorescence Quenching upon Binding to the Receptor. Quenching of the fluorescence of the peptide ligand after

[2] Fluorescent lifetimes of the peptides were determined on an SLM 4800C spectrofluorometer by either modulation (m) or phase (p) measurements at 30 MHz and are expressed as the average values (in ns) of multiple determinations: tetrapeptide 3.72 ± 0.13 (m), 3.67 ± 0.23 (p); pentapeptide 3.64 ± 0.10 (m), 3.68 ± 0.23 (p); hexapeptide 3.68 ± 0.12 (m), 3.66 ± 0.20 (p).

Table I: A Comparison of Peptide Quenching As Determined by Cytometric and Fluorometric Methods[a]

method	peptide	n	I_b/I_f
cytometric	tetra	5	0.72 ± 0.05
	penta	5	0.54 ± 0.04
	hexa	5	1.00
fluorometric	tetra	11	0.71 ± 0.06
	penta	5	0.55 ± 0.07
	hexa	6	1.00 ± 0.00

[a] Cytometric data were analyzed as described in the text, and fluorometric data were obtained and analyzed as explained in Figure 1. Individual quenching values are the means calculated from multiple determinations. Cytometric analysis of I_b/I_f for the hexapeptide in all cases was taken to be equal to 1.00, on the basis of fluorometric data, and thus underwent no statistical analysis. In all cases, 10 nM peptide was used ($\sim 25 \times K_d$) providing for the apparent saturation of the high-affinity binding sites.

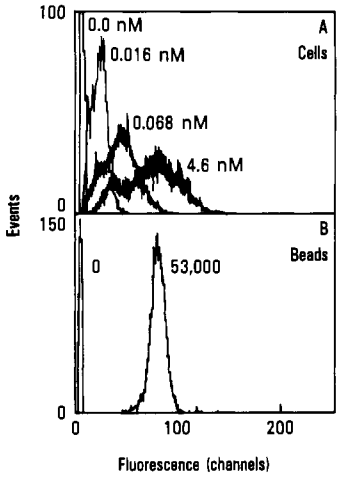

FIGURE 2: Cytometric comparison and calibration at equilibrium of bound fluorescent peptide with standard fluorescent beads. (A) Pentapeptide at concentrations of 0, 0.016, 0.068, and 4.6 nM was bound to permeabilized neutrophils by the standard equilibrium binding assay and analyzed via flow cytometry. (B) With the same cytometer settings as used with the cells, standards beads containing 0 fluorescein equivalents/bead or 5.3×10^4 fluorescein equivalents/bead were analyzed cytometrically for fluorescence. From this comparison, receptors bound/cell can be calculated as explained under Materials and Methods.

binding to the receptor was determined both cytometrically and fluorometrically as shown in Table I. The intensity of bound ligand relative to free ligand (I_b/I_f) is unique for each of the ligands, and there is excellent statistical agreement between the values determined by the two independent methods. The fluorometric method (Figure 1) relies upon a direct observation of quenching upon binding. In contrast, the cytometric method depends upon the assumption that the absolute number of sites available to each of the ligands is identical at saturation of the receptors. Peptide-dependent differences in cell-associated fluorescence at saturation, as determined by equilibrium binding experiments as shown in Figure 3, permitted direct measurement of relative quenching. The equivalence of the two methods implies comparable quantum yields (Q_r) prior to binding.

Quantitation of Bound Receptor. The quantitation of cellular receptor binding by flow cytometry is shown in Figure 2. In panel A of this figure, increasing fluorescent peptide concentration increases cell labeling (from left to right; peaks 2, 3, and 4) over cell autofluorescence (peak 1). Cytometric analysis of standard beads (Figure 2, panel B) permits the calculation of the average amount of bound receptor per cell (eq 1).

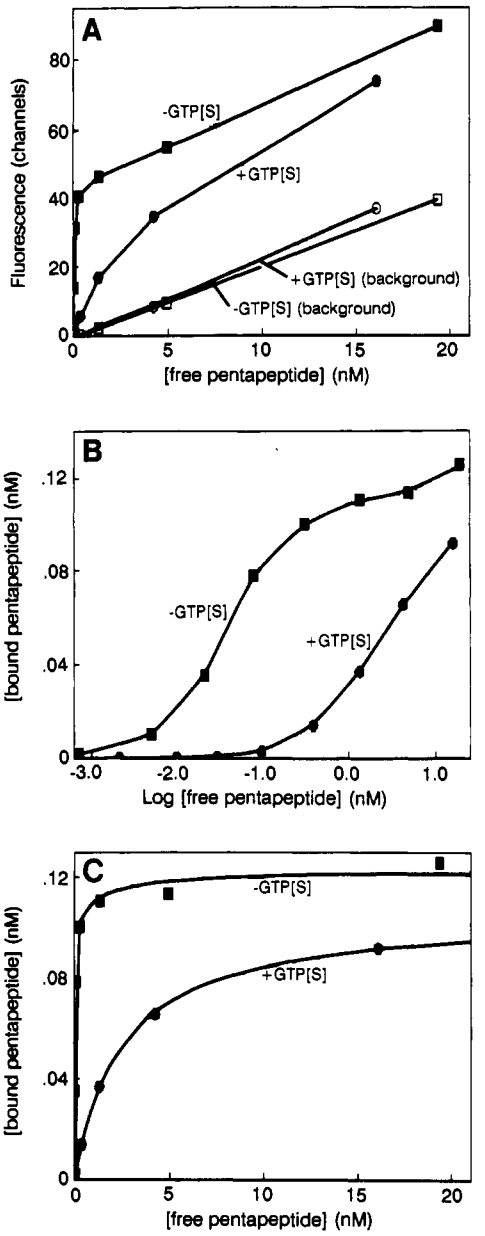

FIGURE 3: Pentapeptide equilibrium binding to permeabilized neutrophils. (A) Pentapeptide, in a concentration range from 0.01 to 30 nM, was bound to cells (10^6/mL) in the presence or absence of the blocking peptide and GTP[S] and analyzed as described for the standard equilibrium binding reaction. The total amount of bound pentapeptide (expressed as channel number) was plotted as a function of the concentration of the total peptide in the reaction. (B) The amount of bound pentapeptide, corrected for background, was calculated as explained under Materials and Methods and graphed as a function of the log of the free pentapeptide concentration at equilibrium. The concentration of the free pentapeptide concentration at equilibrium. The concentration of the free pentapeptide in the reaction was determined as explained under Materials and Methods. (C) The net amount of pentapeptide bound was calculated and graphed as a function of the free pentapeptide concentration at equilibrium. The single-site fit for the data of the experiment shown in the figure in the presence of nucleotides gave a K_d of 2.53 nM and 66 000 sites. In the absence of nucleotides, there were 66 000 sites with a K_d of 0.04 nM and 6000 sites with a K_d of 2.53 nM.

Equilibrium Binding in the Presence and Absence of Guanine Nucleotide

The binding of the pentapeptide to permeabilized neutrophils was analyzed cytometrically as shown in Figure 3. The results are representative of three separate experiments. Panel A shows raw channel numbers for binding as a function of ligand concentration. There is higher affinity binding in the absence

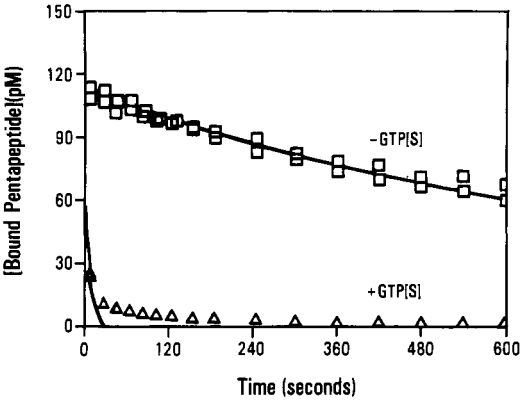

FIGURE 4: Kinetic analysis of pentapeptide dissociation from permeabilized neutrophils. The cytometrically monitored kinetic release of the pentapeptide was performed with permeabilized neutrophils prebound to equilibrium with 0.5 nM pentapeptide. At $t = 0$ s, cells were diluted 10-fold into IBB containing either the blocking peptide alone (□) or the blocking peptide and GTP[S] (△), quickly vortexed, and immediately analyzed for their fluorescence. Initial levels of bound peptide were determined by diluting bound cells at equilibrium into IBB alone, while values for background fluorescence were determined by diluting blocked cells in the presence of peptide into IBB. Analysis of triplicate determinations yielded k_{off} values of $1.06 \times 10^{-3} \pm 0.04 \times 10^{-3}$ and $1.43 \times 10^{-1} \pm 0.04 \times 10^{-1}$ s^{-1} in the presence and absence of nucleotide, respectively.

of GTP[S]. The blocking protocol was equally effective in both the presence and absence of guanine nucleotides, and the nonspecific contribution is nearly linear with concentration. Ligand binding was corrected for background fluorescence, expressed as the concentration of bound pentapeptide, and was plotted in panel B vs the log of the free pentapeptide concentration. No high-affinity binding is retained in the presence of GTP[S], and the data reveal a second lower affinity site of pentapeptide binding in the absence of GTP[S].

The data were fit to single sites in the presence and two independent sites in the absence of guanine nucleotide. Averaging two experiments, there are 69 000 ± 3000 low-affinity sites per cell in the presence of nucleotides with a K_d of 2.6 ± 0.1 nM. In the absence of nucleotides, there are ~66 000 sites per cell with a K_d of 0.04 ± 0.01 nM. If the K_d of the low-affinity sites in the absence of nucleotides, is fixed to 2.6 nM, there are ~15 000 low-affinity sites.

Kinetics of Peptide Binding

Measurements of ligand dissociation by cytometric methods are shown in Figure 4. The dissociation halftime is ~650 s in the absence of nucleotides. Analysis of triplicate determinations yielded a rate constant of $1.06 \times 10^{-3} \pm 0.04 \times 10^{-3}$ s^{-1}. In the presence of nucleotides, the dissociation of ligand is rapid from a large fraction of receptors that are nucleotide sensitive. Analysis of triplicate determinations of these data yielded a rate constant of $1.43 \times 10^{-1} \pm 0.04 \times 10^{-1}$ s^{-1}. Previous reports of the use of antibody methodology to measure dissociation (3–8 s) and more accurate analysis by using the restoration of ligand intensity following release from the receptor (4–6 s, Sklar et al., 1990) are consistent with an off-rate constant of ~0.15 s^{-1}.

The kinetics of pentapeptide binding to permeabilized neutrophils were analyzed cytometrically as shown in Figure 5. Representative histograms and time courses of binding from a single experiment repeated three times are shown in panels A and B. Data corrected for the contribution of nonspecific binding (triangles and solid line in panel B) are plotted in panels C and D and reflect kinetics in the absence or the presence of GTP[S]. The approach to equilibrium in the

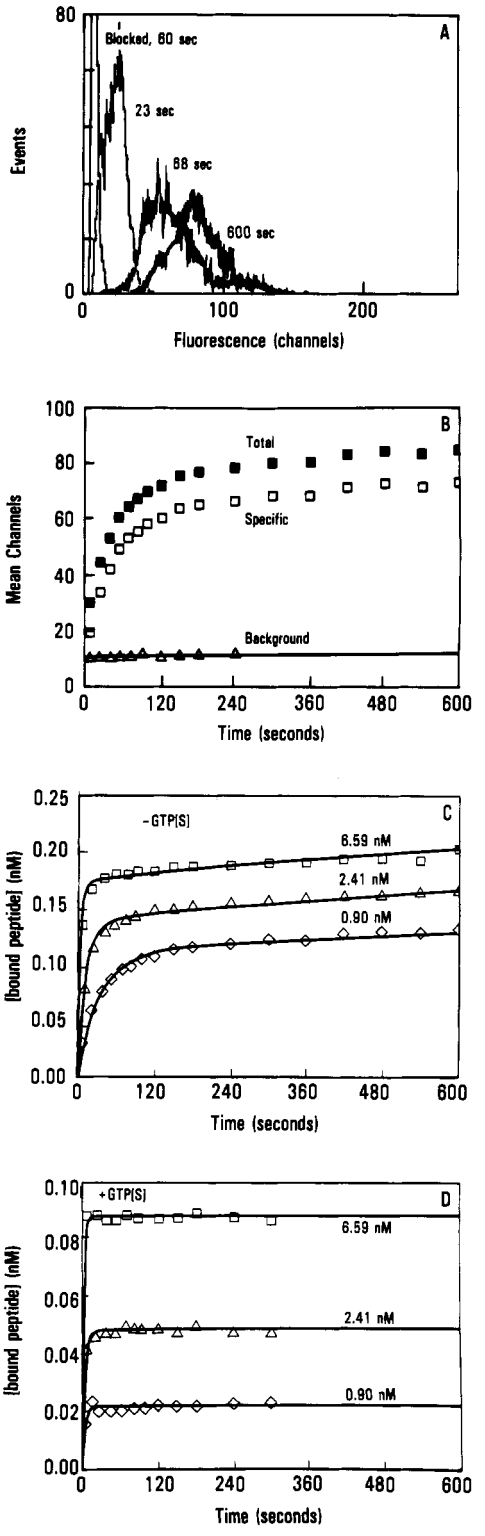

FIGURE 5: Kinetic analysis of pentapeptide binding to permeabilized neutrophils. (A) Data acquisition in kinetic cytometric binding reactions with the pentapeptide at a final concentration of 0.90 nM was added to cells (10^6/mL) at $t = 0$ s. At 23, 68, and 600 s (in the presence and absence of the blocking peptide), 2000 cells were analyzed for their fluorescence and expressed as channel number. (B) Channel number vs time, showing correction for background fluorescence. At $t = 0$ s, the pentapeptide at a final concentration of 0.90 nM was added to cells alone (■) or to cells in the presence of the blocking peptide (△), kinetic binding data being collected at the indicated times. The blocked data were modeled as described and subtracted from the nonblocked data to yield specific pentapeptide bound (□). Duplicate analyses were averaged (C) in the absence or (D) in the presence of GTP[S], displayed as [receptor bound] vs time, and modeled. The final concentrations of the pentapeptide were 6.59 (□), 2.41 (△), or 0.90 nM (◇).

absence of nucleotides is slow (panel C) and dependent on the ligand concentrations that are in excess of those of the receptor and approach saturation. In the presence of nucleotides (panel D), binding plateaus rapidly and at levels less than saturation.

As seen in Figure 5D, the association behavior of ligand in the presence of nucleotides is adequately fit by single-step reversible binding. The on-rate and the off-rate constants (k_{+1}, k_{-1}) are 2.84×10^7 M^{-1} s^{-1} and 0.158 s^{-1}, respectively, the K_d calculated from the kinetic analysis is 5.6 nM (at 37 °C) compared to the K_d of 2.6 nM (at room temperature) based on the equilibrium measurements. Simultaneous fits to the data in the absence of nucleotides yielded these observations. Models II and III were judged inadequate because of systematic errors and large χ^2 values (5.0×10^{-3} and 2.6×10^{-3}). Models IV and V were judged inadequate both because of systematic errors, χ^2 values (2.0×10^{-3} for IV and 1.2×10^{-3} for V), and predicted off-rate constants (9.7 s^{-1} and 0.006 s^{-1} for IV and 16 s^{-1} and 0.003 s^{-1} for V). Models VI and VII both fit the data (χ^2, values: 7.4×10^{-4}; 1.1×10^{-3}) with little systematic error and predict equilibrium and dissociation behavior consistent with that observed.

Model VI provides two classes of receptors, one precoupled to G and the other finding G in a separate step. The values of the variables for the data set shown are the total receptor concentration (0.24 nM); the fraction of RG (= 44%); the rates at which ligand binds ($k_{+1} = 2.8 \times 10^7$ s^{-1}) and dissociates from each form ($k_{-1} = 0.17$ s^{-1} for LR, k_{-3} fixed according to Figure 4 at 1.06×10^{-3} s^{-1}, yielding a calculated net dissociation in the absence of nucleotides of 7.5×10^{-4} s^{-1}); and the interconversion rates between the two forms ($k_{+2} = 1.9 \times 10^{-3}$ s^{-1} and k_{-2} was vanishingly small). Averaging three independent experiments, the k_{+1} values were $3.35 \times 10^7 \pm 1.03 \times 10^7$ s^{-1} M^{-1}, and the k_{-1} values were $1.61 \times 10^{-1} \pm 0.60 \times 10^{-1}$ s^{-1}. In two other experiments, the receptor concentration was ~0.1 nM, similar to the equilibrium experiments. The fraction of RG averaged 52% with a range of 42–71%; the rate of formation of LRG from LR (k_{+2}) ranged from ~0.002 to 0.01 s^{-1}, while the reverse rate was typically two orders of magnitude smaller. The predicted number of receptors in the presence of nucleotides averaged 83% of those determined in the absence of nucleotides.

Model VII provides two classes of receptors, one rapidly coupling (38%) and the other slowly coupling to G. For the data of Figure 5, $k_{+1} = 4.1 \times 10^7$ M^{-1} s^{-1}, with $k_{-1} = 0.23$ s^{-1} and $k_{-2} = 0.0025$ s^{-1}. In the calculations, k_{+2} tended to become very large, suggesting instantaneous coupling, while k_{+3} was 0.03 s^{-1}. On the basis of χ^2, predicted off rates, number of parameters, and the behavior of k_{+2}, Model VI appears to be the more appropriate description of the data.

Discussion

Real-Time Approaches to Ternary Complex Dynamics. Signal transduction during cell activation is a subsecond process. In neutrophils, for example, an elevated level of intracellular calcium is detected in seconds following formyl peptide binding via a receptor–G protein–PI turnover cascade. Phototransduction is a more impressive process from a dynamic standpoint, both because photoresponse occur within milliseconds and because a single photoreceptor may activate a thousand G proteins in a second. These observations require that ligand binding, receptor–G protein coupling and uncoupling, and G protein activation all occur in a subsecond time frame. This report represents an effort to define a systematic new approach to study ternary complex dynamics in ligand–receptor systems. The approach begins with the description of methodology suitable to a real-time analysis of both equilibrium and dynamic ternary complex interactions by fluorescence methods and extends to the characterization of a system in which high- and low-affinity receptor states are readily identified.

Calibration. Calibration methodology is central to any effort to examine binding interactions. While these methods are well-defined for radioligand assays, there have been relatively few membrane receptor systems where this has been accomplished for fluorescence, and even less effort has been directed toward cytometric systems that provide exquisite discrimination of free and bound ligand. In retrospect, our first effort to provide calibration procedures (Sklar et al., 1989a) was hindered by the use of standards that were not stable and by an incomplete appreciation of the difficulty in working with hydrophobic reagents that had to survive multiple transfer steps. This present effort has been enhanced by the introduction of commercial standards that can be used for the calibration of both receptor sites and reagents concentrations. We have extended these approaches from a single ligand to a family of peptides, several of which change fluorescence upon interaction with the receptor, and we have provided new methods for evaluating the quantum yield of the ligand relative to the standard and the free ligand relative to the bound form of the ligand. The binding analysis requires knowledge of the concentration of ligand that has actually been delivered to each assay tube. Errors in the calibration lead to errors in the values for total ligand bound. Moreover, systematic errors in free ligand measurement, particularly at low ligand concentration, can produce significant errors in the binding affinity and the shape of the binding curve. With our hydrophobic peptide reagents, we have required verification of the peptide concentrations in individual assays tubes, and we described a simple small-volume assay technique to meet this need.

The Permeabilized Neutrophil as a Model System for Ternary Complex Interactions. Many receptor systems exhibit ligand binding that is regulated by guanine nucleotides including the α_2-adrenergic receptor (Neubig et al., 1985, 1988; Thomsen et al., 1988), the β-adrenergic receptor (De Lean et al., 1980), the muscarinic receptor (Ehlert, 1985; Wong et al., 1986), the D2-dopamine receptor (Wreggett & De Lean, 1984), and the formyl peptide receptor (Sklar et al., 1989a). In most of these membrane systems, the coupling between receptors and G proteins was heterogeneous with a substantial fraction of receptors that formed a ternary complex slowly or not at all. In several preparations containing mixed receptor states such as the α_2-adrenergic receptor (Neubig et al., 1988), β-adrenergic receptor (De Lean et al., 1980; Contreras et al., 1986), and D2-dopamine receptor (Wreggett & De Lean, 1984), binding data have also been analyzed in ternary complex models in which a ligand binds to at least a portion of the receptor in a precoupled state. In contrast, binding data from systems containing muscarinic receptors (Ehlert, 1985; Wong et al., 1986) fit models in which the ligand binds to very little or no receptor in a precoupled state.

We previously reported a semiquantitative characterization of the formyl peptide receptor in the permeabilized human neutrophil where antibodies to fluorescein were used to discriminate free and bound ligand. This is a system in which signal transduction may be incomplete since phosphoinositide hydrolysis following ligand binding to the receptor has not been reported, although stimulated GTPase activity above high background levels similar to that of neutrophil sonicates has been observed (Mueller and Sklar, unpublished). In the absence of guanine nucleotides, dissociation of nonsaturating fluorescent formyl peptide from its receptors on digitonin-

permeabilized neutrophils was several hundred seconds. When nucleotides were added at saturating conditions, a rapid release (half-time 3–8 s) of ligand from 90% or more of the receptors was observed. Rapidly dissociating receptors have also been detected when the cells were ribosylated with pertussis toxin or alkylated with *n*-ethylmaleimide (Sklar et al., in preparation). Consistent with the interpretation of other systems and previous biochemical measurements in intact neutrophils (Sklar et al., 1989a), the high-affinity (slowly dissociating) binding was attributed to the ternary complex LRG and the low-affinity (rapidly dissociating) binding to the binary complex LR. These earlier studies suffered from several deficiencies, including the lack of the description of the number of sites, the equilibrium binding constant, and the association rate constant. The analysis of the dissociation rate constant for the hexapeptide was complicated by the recognition of the receptor-bound ligand by the antibody.

Our first systematic analysis of the equilibrium binding interaction by real-time methods is therefore provided by the more versatile cytometric approach described in this report (Figure 3). In the presence of guanine nucleotides, the receptors are detected as a homogeneous population of ~69 000 sites with K_d ~3 nM. In the absence of guanine nucleotides, a major population of high-affinity sites (K_d ~0.04 nM, 66 000 per cell) coexists with a second site at equilibrium. If the analysis of the second site fixes that K_d at the value for LR, there is reasonable agreement for the total number of sites in the presence or absence of GTP[S].

Kinetic Analysis of Ternary Complex Assembly and Disassembly. A simple reversible model is appropriate for fitting ligand–receptor interactions in the presence of guanine nucleotides. There is agreement between the K_d based on the equilibrium and kinetic measurements, and, moreover, the off-rate constant derived from the association measurements is in remarkably good agreement with direct measurements of the dissociation as analyzed by four different methods (cytometry, antibody detection of dissociating ligand, fluorescence polarization, and restoration of the intensity of the quenched ligand upon release from the receptor).

No simple model adequately describes ligand–receptor interaction when nucleotides are absent. Neither a single site nor independent two-site fits account for all features of the data. Only when more complex interconverting models incorporate heterogeneity in the receptors can the data be fit. In the ternary complex analysis, this heterogeneity takes the form of "coupled" and "uncoupled" receptors. The coupled receptors are physically precoupled or rapidly in contact with G proteins, and the uncoupled receptors gain access to G proteins more slowly or not at all. The coupled receptors (40–50% of the total) form LRG at a rate indistinguishable from the rate at which L binds to R. Computationally, one would not expect to distinguish unambiguously rapid coupling (half-times less than a second) from precoupling of receptors and G proteins. However, Model VI (precoupling) invariably fits the data better than Model VII (rapid coupling) even though there are more variables in the latter model.

It is also noteworthy that the forward rate constants of 3×10^7 M^{-1} s^{-1} are as large as any reported for interactions of molecules of this size with cell-surface receptors (Goldstein et al., 1989). While the diffusion limit is formally 1–1.5 orders of magnitude greater than the rates reported (Koren & Hammes, 1976), the reduction of the rate constants that restrict the entry of a small molecule into a binding pocket. Taken together however, the kinetic and static binding measurements point to the difference in affinity between LR and LRG as arising principally from the change in the dissociation rate constants.

Implications of Coupling Heterogeneity. Several aspects of the results of the computations are noteworthy in the context of ternary complex models, particularly the speed and heterogeneity of the coupling process. Though not necessarily identical processes, LR and LRG assemble with a very similar rate constant either because R and G coupling are fast compared to ligand binding or because R and G are precoupled. Both interpretations are consistent with the notion that transduction can occur in a subsecond time scale and that the diffusion of R and G in two dimensions in the membrane bilayer also occur in a subsecond time scale. Both the precoupled and the uncoupled models require fast steps. It has been suggested, though not shown directly prior to activation, that G proteins bind endogenous GDP. In either the precoupled or the uncoupled models, endogenous GDP is presumed to be released as a prerequisite for the stabilization of the ternary complex (LRG). To fit single-site kinetics of LR formation, both models would require the rapid release of bound GDP, the uncoupled model requiring rapid coupling as well. In either model, LR formation would require the formation of LRG–GDP, the release of endogenous GDP, the binding of GTP[S], and the disassembly of quaternary complex (LRG–GTP[S]) all without appreciable delay. Thus, rapid formation of either LR or LRG would require not only rapid assembly but, in the case of LR, rapid disassembly of the ternary complex. Rapid interconversions between LRG and LR (a disassembly elicited by GTP[S]) are suggested by the data of Figure 4. Preliminary analysis of the disassembly of LRG is consistent with subsecond nucleotide binding and subsecond quaternary complex stability (Sklar, 1987; Sklar et al., 1989b).

In neutrophil physiology, it has been recognized that there is temporal heterogeneity in cell responses to a ligand. For instance, actin polymerizes and depolymerizes in ~20 s, then repolymerizes, all in response to a single high concentration of the formyl peptide. A possible signal for this response, the G protein dependent generation of PIP_3 follows the same pattern (Eberle et al., 1990). In contrast, responses initiated by the leukotriene B_4 and platelet-activating factor receptors are all short lived. These results could be explained on the basis of heterogeneous receptor coupling suggested by the permeabilized cell if transduction via the other classes of receptors makes use of precoupled forms while formyl peptide receptors involved both precoupled and slowly coupling (minutes) forms. In fact, we previously reported the existence of rapidly dissociating formyl peptide receptors identified as LR in the early seconds of cell activation that disappeared within minutes of ligand binding (Sklar et al., 1989b).

Flow Cytometric Analysis of Ternary Complex Dynamics. While both the general limitations and advantages of flow cytometric methods for ligand receptor analysis have been addressed previously (Sklar et al., 1984, 1989b; Sklar, 1987), there are several unique features relating to the permeabilized cell and ternary complex analysis. A notable aspect is that LR interactions, even though short lived, can be resolved. This is notable because the dissociation half-time of 3–5 s is short enough that radioligand assays could suffer from a significant loss of bound ligand during the wash step. In a homogeneous assay, this appears not to be a significant problem, and we routinely detect comparable numbers of receptors in preparations with and without guanine nucleotides. An additional factor for working with permeabilized cells is the fact that the total cell-associated fluorescence arises not only from specific

binding to the cellular receptors but also from the volumes within individual cells. This "nonspecific binding" is linear, as seen in Figure 3, and can be considerable at high ligand concentrations. Finally, while the intrinsic time resolution of cytometric and fluorometric methods can be comparable, it is difficult to inject a sample in commercial cytometers to obtain accurate early time points. More extensive spectrofluorometric analysis of binding requires stopped-flow mixing and ligands that change quantum yields upon binding. Improved analytical possibilities, and thus the ability to evaluate complex modeling schemes, should make it possible to address directly mechanistic issues regarding precoupling or rapid assembly of R and G, the rates of nucleotide binding to the ternary complex, and the lifetime of the quaternary complex prior to G protein activation.

ACKNOWLEDGMENTS

We thank Dr. A. Kleinfeld for the use of the SLM 4800 for fluorescence lifetime measurements, Dr. H. Motulsky for helpful comments, Dr. B. Goldstein for assistance with the computation, and Dr. R. Freer for a gift of the fluorescent pentapeptide.

Registry No. GTP[S], 37589-80-3.

REFERENCES

Contreras, M. L., Wolfe, B. B., & Molinoff, P. B. (1986) *J. Pharmacol. Exp. Ther. 239*, 136–143.

De Lean, A., Stadel, J. M., & Lefkowitz, R. J. (1980) *J. Biol. Chem. 255*, 7108–7117.

Eberle, M., Traynor-Kaplan, A., Sklar, L. A., & Norgauer, J. (1990) *J. Biol. Chem. 265*, 16725–16729.

Ehlert, F. J. (1985) *Mol. Pharmacol. 28*, 410–421.

Flow Cytometry Standards Corporation (1988) *Monograph: Fluorescent Microbead Standards*, Flow Cytometry Standards Corporation, Research Triangle Park, NC.

Goldstein, B., Posner, R. G., Torney, D. C., Erickson, J., Holowka, D., & Baird, B. (1989) *Biophys. J. 56*, 955–966.

Haugland, R. P. (1989) in *Handbook of Fluorescent Probes and Research Chemicals*, Molecular Probes, Eugene, OR.

Kim, M., & Neubig, R. R. (1985) *FEBS Lett. 192*, 321–325.

Koren, R., & Hammes, G. G. (1976) *Biochemistry 15*, 1165–1171.

Lad, P. M., Olson, C. V., & Smiley, P. A. (1985) *Proc. Natl. Acad. Sci. U.S.A. 82*, 869–873.

Lee, T. W. T., Sole, M. J., & Wells, J. W. (1986) *Biochemistry 25*, 7009–7020.

Levison, S. A., Hicks, A. N., Portman, A. J., & Dandliker, W. B. (1975) *Biochemistry 14*, 3778–3786.

Mercola, D. A., Morris, J. W. S., & Arquilla, E. R. (1972) *Biochemistry 11*, 3860–3874.

Motulsky, H. (1987) ISI Software, Philadelphia, PA.

Muthukumaraswamy, N., & Freer, R. J. (1987) *Methods Enzymol. 162*, 132–139.

Nash, T. (1958) *J. Phys. Chem. 62*, 1574–1578.

Neubig, R. R., Gantzos, R. D., & Brasier, R. S. (1985) *Mol. Pharmacol. 28*, 475–486.

Neubig, R. R., Gantzos, R. D., & Thomsen, W. J. (1988) *Biochemistry 27*, 2374–2384.

Okajima, F., Katada, T., & Ui, M. (1985) *J. Biol. Chem. 260*, 6761–6768.

Pesce, A. J., Rosen, C. G., & Pasby, T. L. (1971) in *Fluorescence Spectroscopy*, Marcel Dekker Inc., New York.

Sklar, L. A. (1987) *Annu. Rev. Biophys. Biophys. Chem. 16*, 479–506.

Sklar, L. A., Finney, D. A., Oades, Z. G., Jesaitis, A. J., Painter, R. G., & Cochrane, C. G. (1984) *J. Biol. Chem. 259*, 5661–5669.

Sklar, L. A., Bokoch, G. M., Button, D., & Smolen, J. E. (1987) *J. Biol. Chem. 262*, 135–139.

Sklar, L. A., Mueller, H., Omann, G., & Oades, Z. (1989a) *J. Biol. Chem. 264*, 8483–8486.

Sklar, L. A., Mueller, H., Swann, W. N., Comstock, C., Omann, G. M., & Bokock, G. M. (1989b) *ACS Symp. Ser. 383*, 52–69.

Sklar, L. A., Fay, S. P., Seligmann, B. E., Freer, R. J., Muthukumaraswamy, N., & Mueller, H. (1990) *Biochemistry 29*, 313–316.

Smolen, J. E., Stoehr, S. J., Traynor, A. E., & Sklar, L. A. (1987) *J. Leukocyte Biol. 41*, 8–13.

Thomsen, W. J., Jacquez, J. A., & Neubig, R. R. (1988) *Mol. Pharmacol. 34*, 814–822.

Tolley, J. O., Omann, G. M., & Jesaitis, A. J. (1987) *J. Leukocyte Biol. 42*, 43–50.

Wong, H. M. S., Sole, M. J., & Wells, J. W. (1986) *Biochemistry 25*, 6995–7008.

Wreggett, K. A., & De Lean, A. (1984) *Mol. Pharmacol. 26*, 214–227.